Video Article

A TIRF Microscopy Technique for Real-time, Simultaneous Imaging of the TCR and its Associated Signaling Proteins

Travis J. Crites[1], Lirong Chen[1], Rajat Varma[1]

[1]Laboratory of Cellular and Molecular Immunology, National Institute of Allergy and Infectious Diseases, National Institutes of Health

Correspondence to: Rajat Varma at varmarajat@mail.nih.gov

URL: http://www.jove.com/video/3892
DOI: doi:10.3791/3892

Keywords: Immunology, Issue 61, Gene delivery, primary cells, T cells, fluorescence microscopy, total internal reflection fluorescence, T cell receptor, signaling

Date Published: 3/22/2012

Citation: Crites, T.J., Chen, L., Varma, R. A TIRF Microscopy Technique for Real-time, Simultaneous Imaging of the TCR and its Associated Signaling Proteins. *J. Vis. Exp.* (61), e3892, doi:10.3791/3892 (2012).

Abstract

Signaling is initiated through the T Cell Receptor (TCR) when it is engaged by antigenic peptide fragments bound by Major Histocompatibility Complex (pMHC) proteins expressed on the surface of antigen presenting cells (APCs). The TCR complex is composed of the ligand binding TCRαβ heterodimer that associates non-covalently with CD3 dimers (the εδ and εγ heterodimers and the ζζ homodimer)[1]. Upon engagement of the receptor, the CD3 ζ chains are phosphorylated by the Src family kinase, Lck. This leads to the recruitment of the Syk family kinase, Zap70, which is then phosphorylated and activated by Lck. After that, Zap70 phosphorylates the adapter proteins LAT and SLP76, initiating the formation of the proximal signaling complex containing a large number of different signaling molecules[2].

The formation of this complex eventually results in calcium and Ras-dependent transcription factor activation and the consequent initiation of a complex series of gene expression programs that give rise to T cell differentiation[2]. TCR signals (and the resulting state of differentiation) are modulated by many other factors, including antigen potency and crosstalk with co-stimulatory/co-inhibitory, chemokine, and cytokine receptors [3-4]. Studying the spatial and temporal organization of the proximal signaling complex under various stimulation conditions is, therefore, key to understanding the TCR signaling pathway as well as its regulation by other signaling pathways.

One very useful model system to study signaling initiated by the TCR at the plasma membrane in T cells is glass-supported lipid bilayers, as described previously[5-6]. They can be utilized to present antigenic pMHC complexes, adhesion, and co-stimulatory molecules to T cells-serving as artificial APCs. By imaging the T cells interacting with the lipid bilayer using total internal reflection fluorescence microscopy (TIRFM), we can restrict the excitation to within 100 nm of the space between the glass and the cell surface [7-8]. This allows us to image primarily the signaling events occurring at the plasma membrane. As we are interested in imaging the recruitment of signaling proteins to the TCR complex, we describe a two-camera TIRF imaging system wherein the TCR, labeled with fluorescent Fab (fragment antigen binding) fragments of the H57 antibody (purified from hybridoma H57-597, ATCC, ATCC Number:HB-218) which is specific for TCRβ, and signaling proteins, tagged with GFP, may be imaged simultaneously and in real time. This strategy is necessary due to the highly dynamic nature of both the T cells and of the signaling events that are occurring at the TCR. This imaging modality has allowed researchers to image single ligands [9-11] as well as recruitment of signaling molecules to activated receptors and is an excellent system to study biochemistry *in-situ*[12-16].

Video Link

The video component of this article can be found at http://www.jove.com/video/3892/

Protocol

Experimental Procedure:

1. Transfection using Amaxa Mouse T Cell Nucleofector Kit

We describe here the transfection of either naïve or in-vitro activated primary T cells with expression plasmids encoding signaling molecules tagged by GFP, using the Amaxa Mouse T Cell Nucleofector Kit. In-vitro activation of T cells using peptide-loaded splenic APCs is performed as described before[7]. All the T cells used in our studies express the AND TCR that recognizes MCC peptide (88-103) bound to the MHC molecule I-E^k. Transfection is carried out essentially according to the manufacturer's recommendations; however, we present some tips that promote viability of the T cells after transfection. Both viability and transfection efficiency is much higher in in-vitro activated T cells than in naïve cells.

1. Before starting, prepare 2 mL of supplemented T cell medium by adding 20 µL of both medium Components A and B and 100 µL of fetal bovine serum (5%) for each transfection to be performed. Equilibrate the medium in a 12-well plate in a humidified 37 °C, 5% CO_2 incubator for at least an hour. Alternatively, aliquots of medium supplemented with 5% serum and Component A may be prepared and stored frozen. If this is the case, thaw the required number of aliquots, add Component B, and perform the equilibration.

Copyright © 2012 Creative Commons Attribution-NonCommercial-NoDerivs 3.0 Unported License

- Pre-equilibration of the medium is very important, as cell death will result from the re-suspension of cells after transfection in medium that is either cold or has a pH other than 7.2.

2. Next, prepare the transfection mixture. Combine 82 µL of Mouse T Cell Nucleofector Solution with 18 µL of Supplement 2 and 5µg of plasmid DNA (concentration no lower than 0.5 µg/µl). Mix thoroughly by tapping the tube or with the use of micro pipette.

- It is important to perform a titration of plasmid dose for a fixed number of cells for each construct to be used for transfection. For some larger constructs, more DNA may be required. DNA should be free of endotoxins.

3. Transfer 5 to 10 million cells to a 15 mL centrifuge tube. Centrifuge at 600 rpm for 5 minutes at room temperature. Remove as much of the supernatant as possible with a vacuum aspirator.

- The manufacturers recommend spinning the cells at less than 90x g; in our case, this speed corresponds to 75x g. The chosen relative centrifugal force (RCF) to obtain a cell pellet is perhaps the most crucial variable, as centrifugation at low RCF precludes damage to the cell membrane.

4. Re-suspend the cell pellet in the transfection mixture by gently and slowly pipeting the cell pellet until there are no large clumps of cells remaining. This can usually be accomplished by completely aspirating the cells through the pipette tip no more than 3-4 times.
5. Using a pipette, carefully transfer the suspension into a certified Amaxa cuvette, ensuring that there are no bubbles present. Cap the cuvette.
6. Select Nucleofector program X-001 on the Nucleofector device. Insert the cuvette into the Nucleofector Cuvette Holder and apply the selected program.

- After electroporating the cells, it is best to immediately transfer them to the pre-equilibrated culture medium. The manufacturers recommend that the cells be kept in the nucleofector medium for no longer than 15 minutes.

7. Bring the cuvette and the pre-equilibrated, fully-supplemented culture medium to the hood. Using the provided plastic pipette, add approximately 500 µL of the medium to the cuvette and transfer the cell suspension to the medium in the plate drop by drop.
8. Incubate the cells at 37 °C for 4 hours before imaging. Naïve cells are incubated at 30 °C instead of 37 °C. This helps maintain their reactivity to antigen.

- Three to four hours of incubation are generally sufficient for T cells to detectably express the GFP tagged proteins. We chose to image cells at this time point because the level of expression is low and artifacts of over-expression should be minimized. If over-expression of a particular protein is desired, however, T cells should be removed from the Amaxa medium after 4 hours. This is accomplished by again pelletting the cells at low RCF and resuspending in pre-equilibrated T cell culture medium supplemented with 50 U/mL of Interleukin 2 (IL-2) at a density of 2 million cells/mL.

2. TIRF Microscopy

Description of the TIRF microscope:

1. General configuration: Optical components were built around an Olympus IX71 fluorescence microscope that was originally equipped with an Olympus TIRF module. We soon discovered chromatic effects in this module when a single alignment state did not achieve coincident collimation for laser lines of different wavelengths. This module, therefore, would not allow for simultaneous TIRF imaging using different excitation wavelengths, and we set out to construct a custom TIRF apparatus that minimizes chromatic effects in the system, as we discuss in detail in the following sections. The method described here was developed for the 150 X magnification, 1.45 numerical aperture (NA) TIRFM objective (Olympus) but works just as well for the 60 X magnification, 1.45 NA versions. For wide field illumination, the microscope is connected to a metal halide Lambda-XL light source and an excitation filter wheel (Sutter Instruments) fitted with excitation filters. For automated positioning of the sample stage with respect to the objective, the microscope is equipped with a motorized XY translation, piezo-controlled Z stage (ASI). Images are captured using two identical QuantEM electron multiplying (EM) CCD cameras (Photometrics). The pixel size of these cameras matches very well with the magnification offered by the 150 X TIRF objective, giving a final resolution of 0.1 µm per pixel. The EMCCD cameras also offer the sensitivity to visualize GFP transfectants having low expression level.
2. Lasers: For TIRF illumination, a system of 5 lasers delivering a total of 6 laser lines (405, 440, 488, 514, 561 and 640 nm) is coupled into a single-mode fiber (Solamere Technologies). The Argon laser and 561 nm diode pumped solid state (DPSS) laser (lines 488, 514 and 561) are routed through an acousto-optical tunable fiber (AOTF) for intensity control while the intensity of the diode lasers (405, 440 and 640 nm) is controlled by modulating the voltage of their power supplies. The voltage on the AOTF and the power supplies of the diode lasers is controlled through a data acquisition card (DAC) board (Measurement Computing) using MetaMorph software (Molecular Devices). The coupling efficiency for the diode lasers is 30% while those of the Argon and DPSS lasers are approximately 60% due to their smaller beam diameters.
3. TIRF module: In order to simultaneously image the TCR and its associated signaling molecules, as described earlier, it was essential to have TIRF illumination that was chromatically corrected and that would not require realignment or refocusing when acquiring fluorescence emissions of different wavelengths. TIRFM was achieved using through-the-objective illumination, as described before[17]. The fiber optic cable that delivers laser light to the microscope was secured into a fiber launch fitted with an XY fiber holder mounted atop a micrometer-driven optical rail for Z adjustment (Thorlabs). To achieve TIRF illumination, the laser beam is focused at the back focal plane of the objective using a system of two lenses (L1 (collimating lens) and L2 (focusing lens) in **Figure 1**), so that the beam emerges collimated out of the objective. This ensures that all rays of light coming out of the objective will have the same angle with respect to the sample plane. The tip of the optic fiber is positioned at the focus of the collimating lens. By moving the micrometer along the optical rail with respect to the collimating lens (the Z direction) it is possible to adjust the focus of the beam and move the beam in X and Y position using the XY adjustment knobs. Owing to the very small back aperture of the 150 X objective, we found that to achieve TIRF, the size of the laser spot at the back focal plane needed to be small. To achieve the focus necessary to produce the small spot, lenses of short focal length were necessary (Keir Neumann, personal communication); hence, we used a focusing lens with a focal length of approximately 108 mm that was placed in the dichroic cube

Copyright © 2012 Creative Commons Attribution-NonCommercial-NoDerivs 3.0 Unported License

directly preceding the objective. The collimating lens was placed closer to the beam splitter that brought in the TIRF illumination. To minimize unwanted chromatic effects, we used achromatic doublets (chromatically corrected lens made by fusing two lens elements made from materials of different refractive indices) with antireflection coatings for both the collimating and focusing lenses (JML Optical). The focus can be verified by checking that the beam emerges collimated out of the objective when positioned in the center of the back aperture and should form a tight spot on the room ceiling. The position of the focused spot is then moved toward the edge of the aperture (in the Y direction) which causes the beam to converge on the image plane at large angles, and eventually, the critical angle for total internal reflection is achieved. Using these optical components, we achieved simultaneous collimation for all wavelengths from 442 to 640 nm at the same alignment. A single optical alignment, therefore, allowed us to perform TIRFM simultaneously across multiple wavelengths.

4. Dual camera apparatus: Simultaneous acquisition of the distinct fluorescence emission arising from two different fluorophores was achieved by building a dual camera system which splits the emission into two wavelength ranges through the use of dichroic mirrors (**Figure 2**). Emitted light is reflected from the objective out of the right side port of the microscope. As most objectives are infinity corrected (with images formed at infinity), a tube lens is required to focus the image. To manipulate two emission wavelengths simultaneously, the tube lens on the right side port was removed. A customized adapter containing c-mount threads (Sutter Instruments) was attached and linked to a dichroic mirror holder (Edmund Optics). Dichroic mirrors that separate the GFP emission from that of organic dyes used to label the TCR (Alexa546, Alexa647, etc.) were installed in this holder. This module was followed in both light paths by a tube lens holder, an emission filter holder and extension tubes. The tube lenses (TL1 and TL2 (**Figure 2**)) have a focal length of 180 mm. Gaps in the extension tubes leading to the EM CCD cameras were covered with black paper to shield the cameras from stray light. To allow for alignment of the two channels, the cameras were mounted on two custom XYZ translation stands (Holmarc Products).

Below we describe how to align the microscope for two channel simultaneous imaging. The steps involved are aligning the TIRF illumination, adjusting the laser power, and aligning the two output images using sub-resolution microbeads.

1. Before starting, all components of the microscope are powered on. The computer and software are then started and it is ensured that all hardware components are recognized by the software.
2. For use as a co-localization standard, dilute 1 µL of sub-resolution (0.2 µm) Fluoresbrite Multi-fluorescent Microspheres into 2 mL of PBS and add 0.25 mL of the microsphere suspension to each well of a Lab-Tek II 8-well chambered coverglass system (Nunc). Place the chamber slide system onto the platform above the objective. Beads that are adsorbed to the glass are then brought into focus.
3. Using the Y alignment of the XYZ fiber launch, the position of the laser beam is moved to the center of the back aperture of the objective. It is important to do this when the objective is in the position where the glass plane is in focus. If the beam is not collimated, the Z micrometer is adjusted to achieve full collimation. Collimation is tested individually for all the laser lines to be used in the experiment. At this stage, the laser power for each line is measured using a laser power meter and is adjusted to 20-30 µW in each channel.

-T cells are extremely sensitive to laser radiation, and the illumination is limited to a total of 50 µW.

4. Images of the beads are acquired using TIRF illumination in the live mode. Turn the Y-alignment micrometer on the fiber launch so that the beam starts moving away from the ceiling until its angle with respect to the objective's optical axis approaches 90 degrees. Eventually, when the critical angle for TIR is reached, the laser light will no longer exit the objective. TIRF alignment is then judged by focusing up and down through the plane of the coverglass. If beads that are floating in solution may be visualized, then the angle of the beam with respect to the objective normal needs to be increased further. At the correct TIRF alignment, only one optical plane will be in focus (i.e., only the beads that are adsorbed to the coverslip). A finer test of TIRF alignment can be implemented when imaging T cells stained with a surface dye that have spread on a surface. (See point 3.4).
5. After TIRF illumination has been achieved, the two channels may be aligned with respect to one another. Focus on the beads and compare the position of identifiable features in the images produced in both channels. Using the X and Y micrometer screws on one camera stand, bring the relative position of the beads into as close proximity as possible. Save the images from both channels. These images will be used as a co-localization standard to align the two channels.
6. The cameras also need to be aligned so that they are parfocal with respect to one other. This is achieved by acquiring a set of images of the sub-resolution beads that are separated from each other in the Z direction by 100 nm. If the maximum intensity pixel for the beads lies in the same plane for both the cameras, then they are parfocal.

3. Imaging

Once the microscope is set up, the next task is to prepare flow chambers containing glass supported lipid bilayers presenting antigen and adhesion molecules as previously described [6] and then perform TIRFM of transfected T cells interacting with the substrate. The published bilayer protocol[5-6] was followed as published except that the liposomes were not incubated for 20 minutes on the coverglass after the flow chamber was assembled. Instead, HBS-BSA buffer was flowed in the flow cell immediately after assembly.

1. Assemble a flow chamber with planar lipid bilayers formed on the glass cover slip containing Ni-NTA lipids. Adhesion molecules, ICAM-1 (100 molecules/μm^2), and peptide-MHC complexes, MCC loaded I-E^k (5-10 molecules/μm^2), are incorporated in the bilayer via their histidine tags. The costimulatory molecule CD80 is added using a GPI anchor (100 molecules/μm^2).
2. Place the flow cell on the stage of the microscope and stabilize it. Attach the manufacturer supplied heating element on the flow cell to control its temperature. Position the objective on a bilayer and bring the bilayer plane in to focus. Enable heating of the objective and the flow cell to stabilize the temperature of the chamber at 37 °C.
3. Transfected T cells are pelleted after 4 hours of incubation at a speed of 80x g and re-suspended in HBS-BSA buffer and supplemented with 10 µg/mL of H57 Fab or 20 µg/mL of H57 single chain variable fragment (scFv) to label the TCR. The cells are then injected in the flow cells. Imaging is done in the continuous presence of the Fab or scFv due to their high dissociation constant. Their presence in the medium does not significantly increase the background as the TIRF field is very thin.
4. Imaging conditions are set up so that dual channel live acquisition shows a live preview of the TCR and GFP channels that helps in searching for transfected cells. TIRF illumination is confirmed by focusing up the glass plane to detect any lateral membrane staining. If lateral

Copyright © 2012 Creative Commons Attribution-NonCommercial-NoDerivs 3.0 Unported License

membranes do not come in focus then the TIRF alignment is good. Transfected cells are then imaged once or in an image sequence to produce videos.

4. Image Processing and Data Analysis

The software outputs images from the two cameras in a single frame. The output of each camera is 512 x 512 pixels; hence, the output image is 1024 x 512 pixels in size. The images first need to be split into individual frames corresponding to the two cameras. The images of sub-resolution beads from the two channels are overlaid and alignment parameters are determined. A feature specific to our system is a 1 degree rotation of one channel with respect to the other (see **Figure 3**). The most likely source of this rotation is the camera stands. After this rotation further relative linear transformations in X and Y need to be performed to perfectly align the beads with respect to each other. Images of beads are obtained in every experiment to determine the precise parameters to align the two channels. These linear and rotational transformations are then applied to all the images and then they are subject to segmentation algorithms and co-localization analysis.

5. Representative Results

The system described here can be adapted to study signaling downstream of any receptor at the plasma membrane. It is particularly informative in studying TCR signaling because signaling occurs in optically resolved clusters called TCR microclusters or in endosomes as recently described[18]. If signaling occurred in sub-resolution clusters of receptors or in un-clustered receptors additional experiments would have to be done to interpret the data. As mentioned before, the CD3 chains of the TCR complex undergo phosphorylation by Src family kinase Lck upon engagement of the TCR by peptide-MHC complexes. The phosphorylated CD3ζ chain then recruits the Syk family kinase Zap70. Visualizing the recruitment of Zap70 thus reports on the phosphorylation status of CD3ζ chain. The strength of TCR stimulation can be altered by using peptides mutated at the TCR contact residues. Such peptides are called altered peptide ligands (APLs). A representative experiment is shown in **Figure 4** where the agonist peptides robustly recruits Zap70 to TCR microclusters while the lower potency peptide T102L fails to recruit Zap70 to TCR microclusters, demonstrating that the CD3ζ chain is not phosphorylated in this case. We could draw this conclusion because we had to just observe the recruitment of Zap70 to TCR clusters that were easily detected by TIRFM. An automated segmentation algorithm was used to count the number of Zap70 microclusters per cell. Also shown in the supplementary movie is the simultaneous imaging of TCR and Zap70 associated fluorescence. Note the dynamic nature of lamelipodium.

Copyright © 2012 Creative Commons Attribution-NonCommercial-NoDerivs 3.0 Unported License

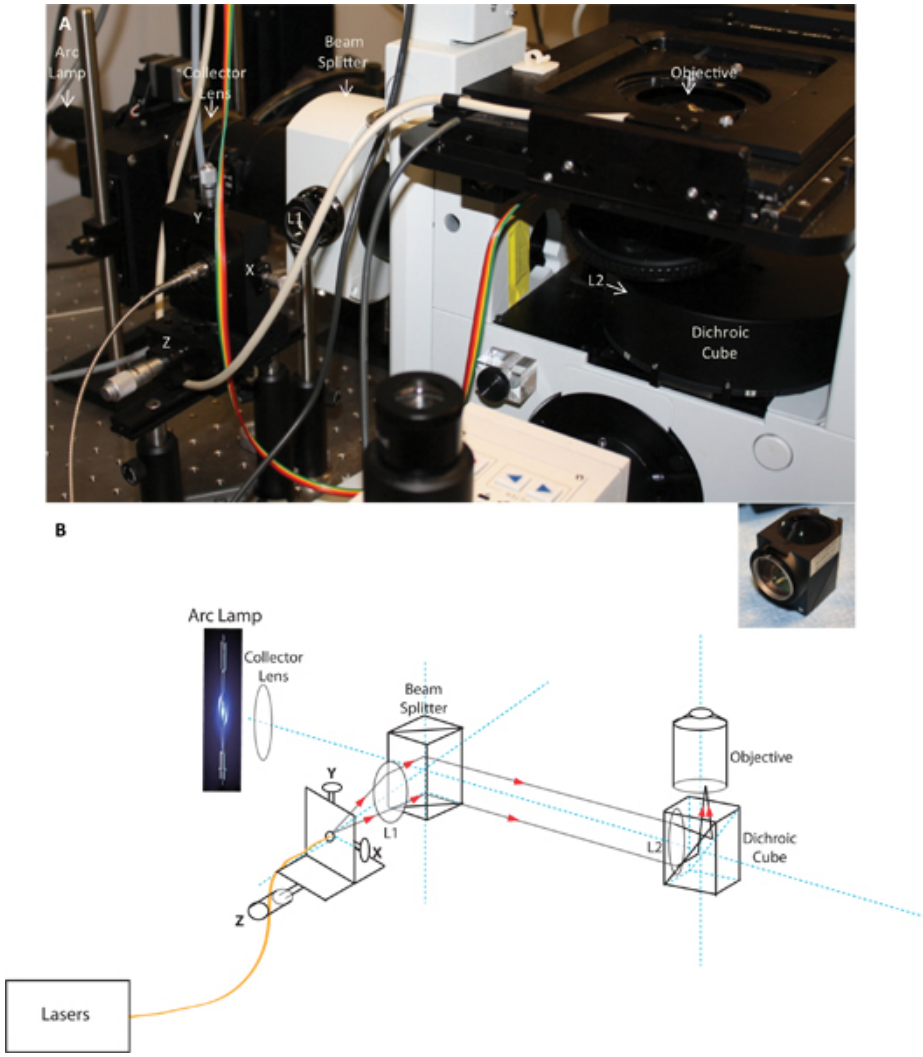

Figure 1. Image and schematic of the custom TIRF launch. Panel A shows the photograph of the TIRF launch as installed on the microscope, and Panel B is a schematic of the TIRF launch demonstrating the light path. The schematic and image showing the position of the collector lens, the beam splitter, the fiber launch with X, Y and Z adjustments, the collimating lens L1, and the focusing lens L2 installed in the dichroic cube and the TIRF objective. The inset shows the focusing lens installed in the dichroic cube.

Copyright © 2012 Creative Commons Attribution-NonCommercial-NoDerivs 3.0 Unported License

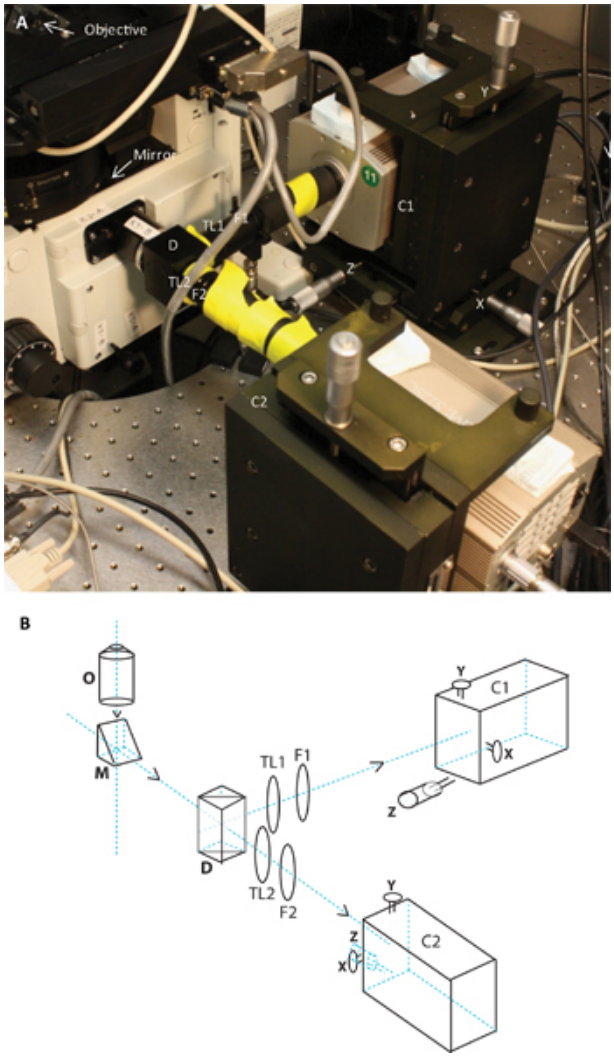

Figure 2. Image and schematic of the two camera system. Panel A shows the photograph of the two camera system as attached to the microscope, and Panel B is a schematic of the same. The schematic and image show the position of the objective, mirror, dichroic, tube lenses TL1 and TL2, emission filters F1 and F2, the two cameras C1 and C2 on their stands with their respective X, Y and Z adjustments.

Copyright © 2012 Creative Commons Attribution-NonCommercial-NoDerivs 3.0 Unported License

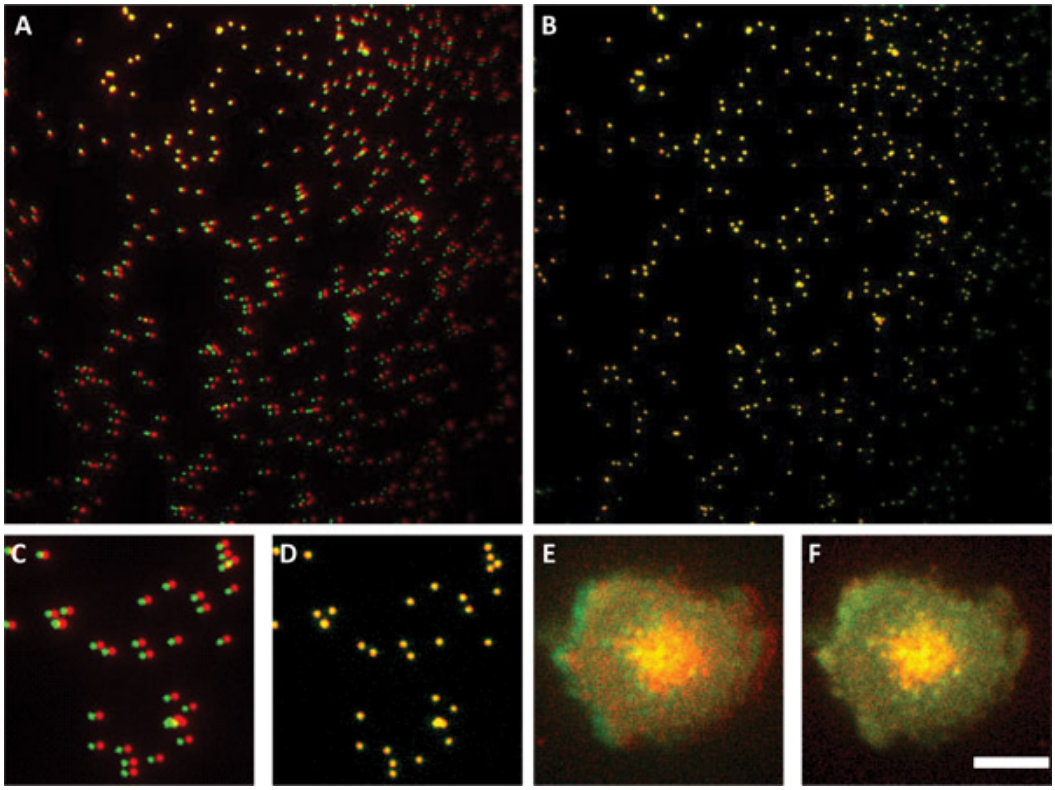

Figure 3. Use of sub-resolution beads to align the two channels. Panels A and B show overlays of sub-resolution beads before (Panel A) and after (Panel B) alignment. Panel A shows that one of the channels is rotated with respect to the other. Panels C and D are a sub section of the images in A and B. Panel E shows a two channel overlay image of cells without processing. Alignment parameters used in panel D were applied to the image shown in panel F. Notice how the lamelipodium from the two channels is perfectly aligned in panel F and not in panel E. Scale bar 4 μm for all the panels.

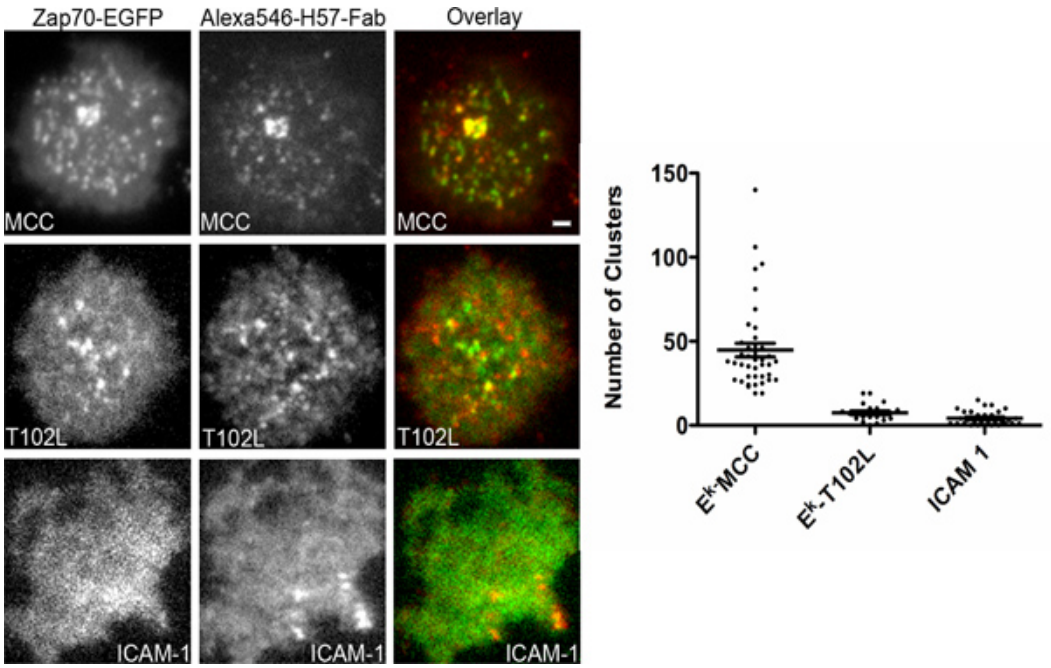

Figure 4. Zap70 recruitment to TCR microclusters in response to different APLs. *In-vitro* activated AND T cells were transfected with a plasmid encoding Zap70 fused to GFP and were incubated on glass supported Ni-NTA bilayers containing 6 molecules/μm^2 of peptide loaded His-tagged-I-E^k, 100 molecules/μm^2 of Alexa647 conjugated His-tagged ICAM-1 and 100 molecules/μm^2 of GPI-anchored CD80. The peptides loaded are indicated in the inset. ICAM-1 refers to cells on bilayers containing 100 molecules/μm^2 of Alexa-647 conjugated His-tagged ICAM-1. Dual channel simultaneous acquisition TIRF microscopy was performed in the continuous presence of Alexa546 conjugated H57 Fab fragment

Copyright © 2012 Creative Commons Attribution-NonCommercial-NoDerivs 3.0 Unported License

(non-blocking) to stain the TCR. Cells were imaged up to one hour after initial contact with the bilayer. Numbers of Zap70 clusters per cell were analyzed using an automated cluster counting software. At least 40 cells were analyzed in each case. Scale bar 2 μm for all the images.

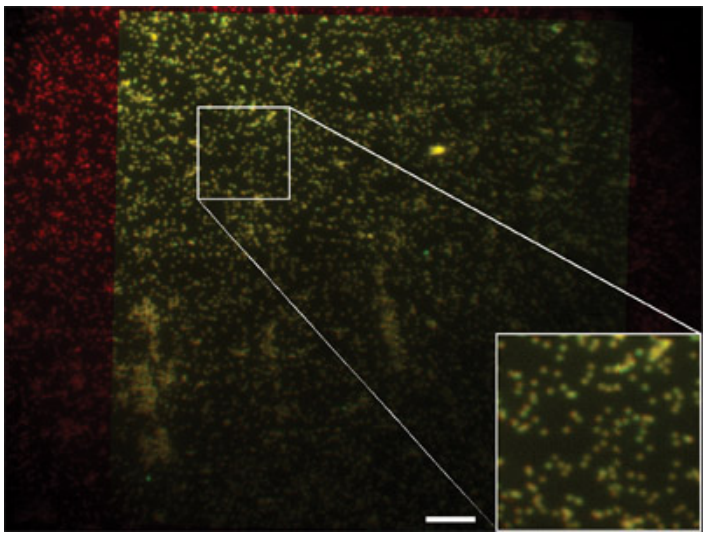

Figure 5. Alignment of the two camera system using two different types of cameras. This panel shows the aligned overlay of sub-resolution beads imaged using the two camera system where the two cameras have different pixel sizes (Green: 6.45 μm pixel size imaged at 2x2 binning and Red: 16 μm pixel size imaged at no binning). Inset shows the magnified view of the square box in the center of the field. Scale bar 5 μm.

Supplementary Movie. Zap70 recruitment to TCR microclusters in response to agonist peptide. In-vitro activated AND T cells were transfected with a plasmid encoding Zap70 fused to GFP and were incubated on glass supported Ni-NTA bilayers containing 6 molecules/μm^2 of peptide loaded His-tagged-I-E^k, 100 molecules/μm^2 of Alexa647 conjugated His-tagged ICAM-1 and 100 molecules/μm^2 of GPI-anchored CD80. Dual channel simultaneous acquisition TIRF microscopy was performed in the continuous presence of Alexa546 conjugated H57 Fab fragment (non-blocking) to stain the TCR. A field of transfected cells was repeatedly imaged 40 times with a time resolution of 10 seconds per frame. Scale bar 2 μm. Click here to view supplementary movie.

Discussion

We describe here a system to study signaling in antigen-specific primary mouse T cells using TIRFM and glass supported lipid bilayers as artificial APCs. The technique relies on successfully expressing GFP tagged proteins in these cells. Transfecting T cells is always a challenging task. Typically, electroporation or gene delivery using retroviruses or lentiviruses are used. One technique is not superior over the other; both have their limitations and advantages. We find that electroporation has the following advantages: 1) It is not required that the cells be actively dividing as is required for retroviruses but not lentiviruses, and 2) The expression level can be controlled by varying the time the cells are incubated before imaging. The biggest drawback is that we find it very difficult to express proteins that are large in size in primary cells. We have presented a method that gives us very good cell viability after electroporation. As a result it is applicable to using it to achieve siRNA mediated gene silencing.

We also describe here a customized two channel simultaneous acquisition TIRF microscope that is chromatically corrected and does not require separate alignment for different wavelengths. These capabilities; however, are available commercially. Our system is based on principles of TIRF microscopy published by experts in the field and is cheaper than commercial alternatives. One possible criticism of our design is that we are using the same angle of incidence for the different excitation wavelengths. This would result in a different TIRF penetration depth for different excitation wavelengths. We think that these effects are small because the evanescent wave is an exponentially decaying field and the depth of the TIRF field is a linear function of wavelength. Fluorophores close to the glass surface will experience no difference in laser intensities between the two wavelengths. For fluorophores near the penetration depth, the intensity difference will be 1.3 fold for the two wavelengths 488 and 640 nm and 1.15 fold for the two wavelengths 488 and 561 nm. The same system can be used in conjunction with super resolution techniques that make use of TIRF illumination.

We have also described a two camera system which is custom built. Like the TIRF system, similar apparatuses are also commercially available. Our system offers flexibility to change the filters and dichroics, allowing its use with different combinations of wavelengths. The drawback of our system is the one degree of rotation needed to align the two images. This issue can be resolved by using camera stands that are piezo driven and offer rotational degrees of alignment. We have also successfully implemented a two camera system on this microscope, in which the cameras are different and have different pixel sizes. A system like this would be useful if one needed sensitivity in one channel and a large dynamic range in another, both of which are rarely available in the same camera. We used the Photometrics HQ-2 camera at 2x2 binning giving us an effective pixel size of 12.9 μm with the Photometrics Quant-EM camera which has a pixel size of 16 μm. A 180 mm focal length tube lens was used for the Quant-EM and a 145 mm focal length tube lens was used for the HQ-2 camera. The HQ-2 was controlled using Metamorph software and the Quant-EM was controlled via micro-manager software on a separate computer in external trigger mode. The external trigger was provided to the Quant-EM camera using a digital output of the measurement computing DAC board, which was implemented as an additional shutter in the configure illumination settings of Metamorph. The ratio of the focal lengths of the tube lenses matches the ratio of the effective pixel sizes. A representative alignment is shown in **Figure 5**.

Copyright © 2012 Creative Commons Attribution-NonCommercial-NoDerivs 3.0 Unported License

Disclosures

All animals used in these experiments were maintained in a specific pathogen-free environment, and the experiments were approved by the National Institutes of Health Animal Care and Use Committee.

Acknowledgements

This research was supported by the Division of Intramural Research of the National Institute for Allergy and Infectious Diseases, National Institutes of Health. We are grateful to Johannes Huppa and Mark Davis for providing us with the scFv of H57 used in these studies. RV would like to thank Keir Neumann for helpful discussion during the development of this technique.

References

1. Call, M.E. & Wucherpfennig, K.W. The T cell receptor: critical role of the membrane environment in receptor assembly and function. *Annu. Rev. Immunol.* **23**, 101-125, doi:10.1146/annurev.immunol.23.021704.115625 (2005).
2. Smith-Garvin, J.E., Koretzky, G.A., & Jordan, M. S.T cell activation. *Annu. Rev. Immunol.* **27**, 591-619, doi:10.1146/annurev.immunol.021908.132706 (2009).
3. Bezbradica, J.S. & Medzhitov, R. Integration of cytokine and heterologous receptor signaling pathways. *Nat. Immunol.* **10**, 333-339, doi:10.1038/ni.1713 [pii] ni.1713 (2009).
4. Fraser, I.D. & Germain, R.N. Navigating the network: signaling cross-talk in hematopoietic cells. *Nat. Immunol.* **10**, 327-331, doi:10.1038/ni.1711 [pii] ni.1711 (2009).
5. Dustin, M.L., Starr, T., Varma, R., & Thomas, V.K. Supported planar bilayers for study of the immunological synapse. *Curr. Protoc. Immunol.* **Chapter 18**, Unit 18, 13, doi:10.1002/0471142735.im1813s76 (2007).
6. Vardhana, S. & Dustin, M. Supported Planar Bilayers for the Formation of Study of Immunological Synapses and Kinapse. *J. Vis. Exp.* (19), e947, DOI: 10.3791/947 (2008).
7. Varma, R., Campi, G., Yokosuka, T., Saito, T., & Dustin, M.L. T cell receptor-proximal signals are sustained in peripheral microclusters and terminated in the central supramolecular activation cluster. *Immunity.* **25**, 117-127, doi:10.1016/j.immuni.2006.04.010 [pii] S1074-7613(06)00297-4 (2006).
8. Yokosuka, T., *et al.* Newly generated T cell receptor microclusters initiate and sustain T cell activation by recruitment of Zap70 and SLP-76. *Nat. Immunol.* **6**, 1253-1262, doi:10.1038/ni1272 [pii] ni1272 (2005).
9. Huppa, J.B., *et al.* TCR-peptide-MHC interactions *in situ* show accelerated kinetics and increased affinity. *Nature.* **463**, 963-967, doi:10.1038/nature08746 [pii] nature08746 (2010).
10. Tolar, P. & Pierce, S.K. A conformation-induced oligomerization model for B cell receptor microclustering and signaling. *Curr. Top. Microbiol. Immunol.* **340**, 155-169, doi:10.1007/978-3-642-03858-7_8 (2010).
11. Treanor, B., *et al.* The membrane skeleton controls diffusion dynamics and signaling through the B cell receptor. *Immunity.* **32**, 187-199, doi:10.1016/j.immuni.2009.12.005 [pii] S1074-7613(10)00043-9 (2010).
12. Treanor, B. & Batista, F.D. Mechanistic insight into lymphocyte activation through quantitative imaging and theoretical modelling. *Curr. Opin. Immunol.* **19**, 476-483, doi:10.1016/j.coi.2007.05.009 [pii] S0952-7915(07)00107-0 (2007).
13. Sylvain, N.R., Nguyen, K., & Bunnell, S.C. Vav1-mediated scaffolding interactions stabilize SLP-76 microclusters and contribute to antigen-dependent T cell responses. *Sci. Signal.* **4**, ra14, doi:10.1126/scisignal.2001178 [pii] 4/163/ra14 (2011).
14. Purbhoo, M.A., *et al.* Dynamics of subsynaptic vesicles and surface microclusters at the immunological synapse. *Sci. Signal.* **3**, ra36, doi:10.1126/scisignal.2000645 [pii] 3/121/ra36 (2010).
15. Lasserre, R., *et al.* Ezrin tunes T-cell activation by controlling Dlg1 and microtubule positioning at the immunological synapse. *EMBO. J.* **29**, 2301-2314, doi:10.1038/emboj.2010.127 [pii] emboj2010127 (2010).
16. Balagopalan, L., Sherman, E., Barr, V.A., & Samelson, L.E. Imaging techniques for assaying lymphocyte activation in action. *Nat. Rev. Immunol.* **11**, 21-33, doi:10.1038/nri2903 [pii] nri2903 (2011).
17. Axelrod, D. Chapter 7: Total internal reflection fluorescence microscopy. *Methods Cell. Biol.* **89**, 169-221, doi: 10.1016/S0091-679X(08)00607-9 [pii] S0091-679X(08)00607-9 (2008).
18. Williamson, D.J., *et al.* Pre-existing clusters of the adaptor Lat do not participate in early T cell signaling events. *Nat. Immunol.* **12**, 655-662, doi: 10.1038/ni.2049 [pii] ni.2049 (2011).

Copyright © 2012 Creative Commons Attribution-NonCommercial-NoDerivs 3.0 Unported License